Journal of Molecular Liquids 387 (2023) 122702

Contents lists available at ScienceDirect

Journal of Molecular Liquids

journal homepage: www.elsevier.com/locate/molliq

Thermodynamic insights into Trans-Aconitate interactions with H^+, Cd^{2+}, Mn^{2+}, and Pb^{2+}: Equilibrium constants, enthalpy changes and sequestering ability

Gabriele Lando [a], Clemente Bretti [a,*], Demetrio Milea [a], Concetta De Stefano [a], Olivia Gómez-Laserna [b], Paola Cardiano [a]

[a] Dipartimento di Scienze Chimiche, Biologiche, Farmaceutiche ed Ambientali, CHIBIOFARAM, Università degli Studi di Messina, Viale Ferdinando Stagno d'Alcontres, 31, I-98166 Messina (Vill. S. Agata), Italy
[b] Department of Analytical Chemistry, University of the Basque Country UPV/EHU, Barrio Sarriena S/N, Leioa 48940 Spain

ARTICLE INFO

Keywords:
Sustainable molecules
$pL_{0.5}$
Pure water model
Potentiometry
Thermodynamic parameters
Citric and tricarballylic acid

ABSTRACT

The thermodynamics of interaction of *trans*-aconitate (L^{3-}) with proton, sodium and potassium cations was studied by means of potentiometric titration performed at different temperatures, ionic strengths, and aqueous ionic media (NaCl, KCl and $(C_2H_5)_4NI$). Three protonation constants and corresponding enthalpy changes are reported at infinite dilution together with their dependence parameters on temperature and ionic strength according to van't Hoff and Extended Debye Hückel equations, respectively. Enthalpy changes resulted slightly endothermic at infinite dilution and values decrease with increasing ionic strength. Proton binding resulted always entropic in nature. Weak association constants of Na^+/L^{3-} and K^+/L^{3-} species were determined using the pure water model approach. Formation constants of *trans*-aconitate with Cd^{2+}, Pb^{2+} and Mn^{2+} were determined in $KCl_{(aq)}$ at different ionic strength values and at 298.15 K. Three complex species were found with all metal cations (ML^-, $MHL^0_{(aq)}$, MH_2L^+), whose formation constant values at infinite dilution and at $T = 298.15$ K were log $\beta = 4.54$, 9.94, 13.77 for cadmium, 5.00, 10.57, 14.81 for manganese and 4.97, 10.44, 14.13 for lead. The as found values resulted unexpectedly high. The sequestering ability of *trans*-aconitate towards M^{2+} was evaluated by determining $pL_{0.5}$ (the ligand total concentration required to bind 50% of the metal cation), and the results show that, throughout the investigated pH range, *trans*-aconitate shows the highest sequestering ability towards Mn^{2+}. Data reported in this paper were critically compared to other tricarboxylic acid, namely citric and tricarballylic acid.

1. Introduction

Toxic metals can pollute water sources [1–3] through industrial discharge, agricultural runoff, and leaching from landfills [4] and mining sites [5]. As it is well known, these pollutants can harm aquatic ecosystems and display serious health effects on both humans and wildlife. Analysis of the data reported in the work of Zhou et al. [6], showed a steady increase in the concentration of metal cations, particularly lead, manganese and cadmium, in rivers and lakes. As a matter of fact, once toxic metals reach the environment, due to their non-biodegradability, their removal becomes a key issue.

Traditional approaches for the recovery of metal cations involved chelating agents such as EDTA that is a potential responsible for various negative effects on the environment [7]. Due to its low biodegradability, EDTA showed the tendency to accumulate in the environment, thus favoring the formation of soluble complexes with dangerous metal cations, increasing their bioavailability, and indirectly contributing to the eutrophication of water [8].

Some examples of new sustainable approaches to recover toxic metals from contaminated water sources contemplated the use of living biosorbents [9–11] (algae, fungi, and bacteria), as well as sorbent coming from agricultural waste products [12–14]. These approaches are currently of great interest since such materials efficiently adsorb metal ions and can be easily separated from liquid phases.

Another strategy involved the employment of a new generation of chelating agents, namely discrete molecules with a good sequestering

* Corresponding author.
E-mail address: cbretti@unime.it (C. Bretti).

https://doi.org/10.1016/j.molliq.2023.122702
Received 4 April 2023; Received in revised form 24 July 2023; Accepted 27 July 2023
Available online 29 July 2023
0167-7322/© 2023 The Author(s). Published by Elsevier B.V. This is an open access article under the CC BY-NC-ND license (http://creativecommons.org/licenses/by-nc-nd/4.0/).

ability towards target cations. Compared to traditional chelating agents, such molecules have the advantage of being featured by a good biodegradability, thus they do not accumulate in the environment. Generally, they are naturally occurring species, such as citric or oxalic acid [15,16], or synthesized starting from L-amino acids [17–19].

It is important to note that when dissolved chelating agents or solid biosorbent are used in multicomponent solutions, they may modify the mobility and bioavailability of all metal cations they come into contact with. Moreover, their removing efficiency may change upon experimental conditions such as pH, temperature and ionic strength. Additionally, while on one side they may be effective in removing toxic metals from the environment, they may also display counter effects due to the lowering of essential metal cations (*e.g.*, Ca^{2+}) levels. For these reasons, the evaluation of the thermodynamic properties and the sequestering ability of such sorbents or chelating agents in different experimental conditions should be undertaken to assess a risks/benefits balance before their use for metal ions recovery applications.

Among naturally occurring chelating agents, an excellent candidate to be exploited in metal ions removing from water is *trans*-aconitic acid (H_3L, Scheme 1), a molecule largely present in sugar cane (about 60 % w/w), or that can be isolated from by-products of the sugar industry. It was found that the amount of *trans*-aconitic acid available in the molasses is between 7.1 and 23.4 g kg^{-1} of dry product [20]. As highlighted in the review of Bruni *et al.* [21] aconitic acid has enormous potential in several industrial and biological applications. For instance, it was used for synthesis of polyesters for tissue engineering [22], as a precursor for preparing high performance carbon dots by hydrothermal reaction [23], as bio-derived plasticizer [24], for the chemical conversion to itaconic acid (high value-added compound) [25], as a plasticizing and cross-linking agent to enhance the elastomeric properties of starch-based composite films [26], as a grafting agent for the modification of chitosan [27], and as antioxidant [28].

Recently, due to its ability to form particular architectures with different topologies and to act as multidentate ligand, *trans*-aconitic acid was used as a linker to synthesize metal–organic frameworks (MOFs) for selective carbon dioxide adsorption [29], and in the formation of rare binodal four-connected 3D MOF possessing a moganite topology, in which four connected nodes adopt distorted configurations [30]. Similarly, *trans*-aconitate showed a peculiar feature, compared to other tricarboxylate ligands, such as citric acid (CA) and tricarballylic acid (TCA), to favor strong particle-bridging interactions [31].

However, despite the scientific interest towards aconitic acid is noticeable, a robust study on *trans*-aconitic acid thermodynamics in solution is still missing, except for an investigation on its acid-base properties [32].

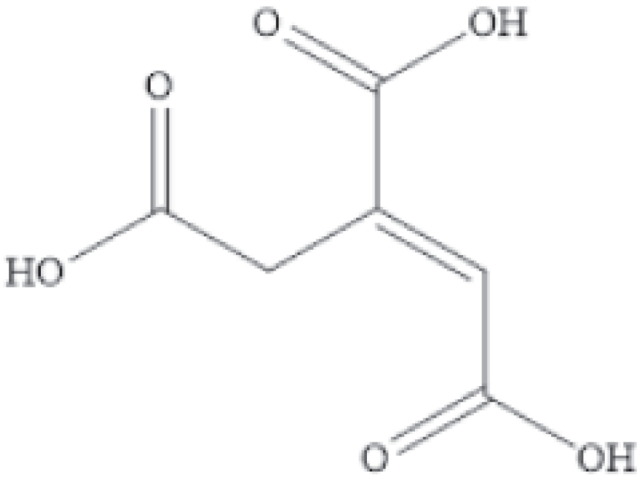

Scheme 1. *Trans*-aconitic acid (H_3L).

As a part of a wider project aimed at carrying out a systematic study on low molecular weight carboxylic acids of environmental interest, in this study the thermodynamic of interaction of *trans*-aconitic acid with proton, sodium and potassium cations are reported, providing data in a standard state (*i.e.*, infinite dilution) and parameters to calculate conditional protonation constants in different ionic media (NaCl, KCl, and $(C_2H_5)_4NI$) at different temperatures and ionic strength values. Moreover, formation constants and sequestering ability of *trans*-aconitate towards environmentally relevant elements (namely Cd^{2+}, Mn^{2+} and Pb^{2+}) are assessed in a wide range of experimental conditions and compared to data reported for other chelating agents.

This study will provide key information to predict the chemistry of *trans*-aconitate in aqueous solutions in different conditions (*i.e.,* pH, medium, etc.) also in the presence of toxic metal cations, so that the best conditions suitable for their selective recovery can be designed. This last aspect is very intriguing since *trans*-aconitic acid is a bio-based compound that can be recovered from a waste biomass, thus allowing a virtuous recycling.

2. Materials and methods

2.1. Chemicals

All chemicals were purchased from Merck (Darmstadt, Germany) at the highest purity available and were used without further purification, except for tetraethylammonium iodide [$(C_2H_5)_4NI$] that was recrystallized from methanol as described by Perrin *et al.* [33]. Potassium hydroxide, sodium hydroxide, tetraethylammonium hydroxide and hydrochloric acid solutions were prepared from concentrated solutions and standardized against potassium hydrogen phthalate (for bases) and sodium carbonate (for acid), previously dried in oven at 383.15 K for 2 h. The concentration of *trans*-aconitic acid in the solutions was determined by alkalimetric titrations. Sodium and potassium chloride solutions were prepared weighing the solid previously dried in oven at 383.15 for 2 h. Metal solutions were prepared weighing the salt and standardized against EDTA. Strong base solutions were stored in dark bottles and soda lime traps were used to prevent dissolution of carbon dioxide. All solutions were freshly prepared, using grade A glassware and twice-distilled water ($\rho \geq 18$ MΩ cm). All chemicals used are listed in Table 1.

2.2. Apparatus and procedure for the potentiometric measurements

Potentiometric titrations were carried out using a Metrohm 809 Titrando equipped with an automatic burette (total volume 10 cm^3) and a combined glass electrode (Metrohm, model 6.0262.100). The estimated accuracy was ± 0.2 mV and ± 0.003 mL for e.m.f. and titrant volume readings, respectively. The apparatus was connected to a PC and controlled by Tiamo 2.5 software to set titrant delivery, data acquisition and to check for e.m.f. stability. All titrations were carried out under magnetic stirring; water presaturated $N_{2(g)}$ was bubbled through the solution to exclude/prevent $O_{2(g)}$ and $CO_{2(g)}$ dissolution. For each measurement aimed to the determination of the ligand protonation constants 25 cm^3 of titrant solution containing suitable amount of *trans*-aconitic acid (analytical concentration, C_L: 1.2 to 6.2 mmol dm^{-3}), $HCl_{(aq)}$ and ionic medium ($NaCl_{(aq)}$, $KCl_{(aq)}$ or $(C_2H_5)_4NI_{(aq)}$) was added to reach pre-established values of pH (~2.0) and ionic strengths ($0.1 \leq I$ / mol $dm^{-3} \leq 1.0$). For the measurements aiming to determine the stability constants of the M^{2+}/L^{3-} systems, MX_2 (X = Cl^- or NO_3^-) (analytical concentration, C_M: 0.7 to 2.6 mmol dm^{-3}, generally, $C_M \leq C_L$) was also added into the cell. The proton analytical concentration (C_H) is the sum of sum of protons coming from HCl plus three times C_L (*trans*-aconitic acid is bearing three protons). For example, in a solution containing H_3L (at $C_L = 5$ mM) and HCl (at a concentration 10 mM), $C_H = 25$ mM. The titrant solutions were titrated with CO_2-free standard base ($NaOH_{(aq)}$, $KOH_{(aq)}$ or $(C_2H_5)_4NOH_{(aq)}$) solutions up to pH ~ 10.0

Table 1
Chemicals used in this work, purchased from Merck (Darmstadt, Germany). Purity (mass) as stated by the supplier.

Chemical	Formula	CAS n°	Purification	Assay (mass)
Sodium chloride	NaCl	7647–14-5	NO	≥ 99%
Potassium chloride	KCl	7447–40-7	NO	≥ 99%
Tetraethylammonium iodide	$(C_2H_5)_4NI$	68–05-3	recrystallisation	98%
Hydrochloric acid	HCl	7647–01-0	NO	≥ 99%
Tetraethylammonium hydroxide	$(C_2H_5)_4NOH$	77–98-5	NO	~10% [a]
Sodium hydroxide	NaOH	1310–73-2	NO	≥ 99%
Potassium phthalate monobasic	$C_8H_5O_4K$	877–24-7	NO	≥ 99.95%
Sodium carbonate	Na_2CO_3	497–19-8	NO	99.995%
Cadmium chloride hydrate	$CdCl_2{\cdot\cdot}H_2O$	654054–66-7	NO	≥ 98%
Manganese (II) chloride tetrahydrate	$MnCl_2 \cdot 4\ H_2O$	13446–34-9	NO	≥ 99%
Lead (II) nitrate anhydrous	$Pb(NO_3)_2$	10099–74-8	NO	≥ 99%
Trans-aconitic acid	$C_6H_6O_6$	4023–65-8	NO	> 98%

[a] Value refers to the concentration in the solutions. On the dry basis, the assay is ≥ 99.5 % (on the mass basis);

or until the electrode started drifting towards lower pH values which indicated the onset of precipitation of sparingly soluble species that are hardly detectable by the naked eye in the initial state.

Before each measurement, the electrode was calibrated in terms of free hydrogen ion concentration [H^+] (not activity) by means of a strong acid (HCl) - strong base ($NaOH_{(aq)}$, $KOH_{(aq)}$ or $(C_2H_5)_4NOH_{(aq)}$) titration in the same pH and ionic strength conditions of the measurement. The fitted parameters in such titrations were E^0 and log K_W (provided in the MS Excel Spreadsheets in supplementary material). Such configuration allowed to convert measured potential (e.m.f.) into pH on a free scale, thus pH = -log[H^+]. Measurements were performed in thermostatted cells at different temperatures (288.15 K, 298.15 K, 310.15 K, and 318.15 K), controlled by a water circulation thermocryostat, model D1-G Haake (uncertainty ± 0.1 K). Further details on the potentiometric measurements are reported in Table 2.

2.3. Calculations

The experimental data represented by titrant volume (cm^3) *vs.* e.m.f. (mV) obtained for all the potentiometric titrations, together with the electrode calibration parameters (E^0 and log K_W), analyzed in this work are reported as supplementary material (MS Excel Spreadsheet), however not all recorded points were used during the data analysis (discarded ones are marked in red). Such experimental data were inputted into the BSTAC4 software [34] together with the mass balance equation of each component involved into the equilibria. The results of the data analysis correspond to the values of the unknown equilibrium constants, expressed as follows:

$$jM^{n+} + i\ H^+ + k\ L^3 = M_jH_iL_k^{(nj+i-3k)} \qquad \beta_{ijk} \qquad (1)$$

where M, H and *L* are the metal cation of interest, the proton and *trans*-aconitate anion, respectively; when $k = 0$ and $i < 0$ eq. (1) refers to metal cation hydrolysis, when $j = 0$, eq. (1) refers to *trans*-aconitate overall protonation constants and are generally indicated as β_i^H. Stepwise protonation constants are indicated as K_i^H (eq. (2).

$$H^+ + H_{i-1}L^{(i-1)-3} = H_iL^{(i-3)} \qquad K_i^H \qquad (2)$$

The conversion from the molar (I_c) to the molal (I_m) concentration scale was performed using the appropriate density values.

The dependence of protonation constants on ionic strength was studied according to two approaches; the first considering the variation of activity coefficients using the extended Debye-Hückel type equation (EDH) and the Specific ion Interaction Theory [35–39] and the second taking into account the formation of weak species between *trans*-aconitate and the ions of the supporting electrolyte using the so-called "Pure water model" [40–44].

A dedicated section containing all the equations used to derive the fitting ones is given as supplementary material. As for the first approach, the ionic strength and temperature dependence of protonation constants was modeled using eq. (3)

$$\log\beta_{ijk} = log^T\beta_{ijk\theta} - z^*_{ijk} \bullet A \bullet \frac{\sqrt{I}}{1 + 1.5 \bullet \sqrt{I}} + \Delta\varepsilon_{ijk} \bullet I + \left({}^T\Delta H^0_{ijk} - z^*_{ijk} \bullet A' \bullet \frac{\sqrt{I}}{1 + 1.5 \bullet \sqrt{I}} + \Delta\varepsilon'_{ijk} \bullet I \right) \bullet \left(\frac{1}{\theta} - \frac{1}{T}\right) \bullet 52.23 \qquad (3)$$

$$z^*_{ijk} = \sum(\text{charge})^2_{\text{react}} - \sum(\text{charge})^2_{\text{prod}} \qquad (3a)$$

$$A = \left(0.51 + \frac{0.856 \bullet (T - 298.15) + 0.00385 \bullet (T - 298.15)^2}{1000}\right) \qquad (3b)$$

$$A' = RT^2 \bullet \ln(10) \bullet \frac{\partial A}{\partial T} = 1.5 + 0.024 \bullet (T - 298.15) \qquad (3c)$$

$$\Delta\varepsilon'_{ijk} = RT^2 \bullet \ln(10) \bullet \frac{\partial \Delta\varepsilon_{ijk}}{\partial T} \qquad (3d)$$

where β_{ijk} and ${}^T\beta_{ijk\theta}$ are the stoichiometric (or conditional) and thermodynamic equilibrium constants at the reference temperature θ = 298.15 K, respectively, $\Delta\varepsilon_{ijk}$ is the summation of the specific interaction coefficients of all the species involved in the equilibrium and the ions of the supporting electrolyte; ${}^T\Delta H^0_{ijk}$ is the enthalpy variation of the equilibrium at infinite dilution; 52.23 is equal to 1/R·ln10, and $\Delta\varepsilon'_{ijk}$ accounts for the ionic strength dependence of protonation enthalpy.

Conventionally, the thermodynamic parameters refer to the molal concentration scale (m = mol $kg(H_2O)^{-1}$), so the symbolism referring to the molar concentration scale are superseded by "c" (*e.g.*, the protonation enthalpy change at infinite dilution in the molar concentration scale is indicated as ${}^T\Delta H^{0c}_{i01}$).

The second approach was applied only to data at 298.15 K and the fitting equation is given in eq. (4):

Table 2
Summary of the potentiometric titrations performed in different ionic media at different temperatures, ionic strength values and at p = 0.1 MPa.

System	medium	T / K	I	C_H [a]	C_L [a]	C_M [a]	n. tit
H^+/L^{3-}	NaCl	298.15	0.1 to 1.0	13 to 28	1.8 to 4.4		12
H^+/L^{3-}	KCl	288.15 to 310.15	0.1 to 1.0	14 to 22	1.2 to 6.2		49
H^+/L^{3-}	$(C_2H_5)_4NI$	288.15 to 310.15	0.1 to 1.0	11 to 22	2.4 to 6.0		11
M^{2+}/L^{3-}	KCl	298.15	0.1 to 1.0	11 to 22	1.1 to 3.7	0.7 to 2.6	45

[a] analytical concentration (mmol dm^{-3}); standard uncertainties (u): $u(T)$ = 0.1 K; $u(I)$ = 0.001 mol dm^{-3}; $u(p)$ = 1 kPa; $u(C_H) = u(C_L) = u(C_M) = 10^{-2}$ mmol dm^{-3}.

$$\log\beta_{ijk} = \log^{T}\beta_{ijk} - A \bullet z^{*} \bullet D.H. + C_{ijk}\cdot I_c + D_{ijk}\cdot I_c^{3/2} + E_{ijk}\cdot I_c^{2} \quad (4)$$

where

$$\text{D.H.} = \frac{\sqrt{I}}{1 + 1.5\cdot\sqrt{I}} \quad (4a)$$

$$C_{ijk} = c_0\cdot p^{*}_{ijk} + c_1\cdot z^{*}_{ijk} \quad (4b)$$

$$D_{ijk} = d_0\cdot p^{*}_{ijk} + d_1\cdot z^{*}_{ijk} \quad (4c)$$

$$E_{ijk} = e_0\cdot p^{*}_{ijk} + e_1\cdot z^{*}_{ijk} \quad (4d)$$

$$z^{*}_{ijk} = \sum(\text{charge})^2_{\text{react}} - \sum(\text{charge})^2_{\text{prod}} \quad (4e)$$

$$p^{*}_{ijk} = \sum p_{react.} - \sum p_{prod} \quad (4f)$$

z and p are the charge and the stoichiometric coefficients of the components of the species, respectively; β_{ijk} can be the protonation constant (β_i^H) or the weak complex formation constant with Na^+ and K^+ (β_{ijk}^M). If the conditions of pure water model hold (see supplementary material and ref. [40]), c_0, c_1, d_0, d_1, e_0, e_1 become constant and are valid for all $M_jH_iL_k$ species (eq. (1)) of the Cd^{2+}/L^{3-} species (including protonation, metal cation hydrolysis) together with their weak complexes (further species that must be included in the new model) with ions of the supporting electrolytes (*i.e.*, Na^+, K^+, Cl^-),

The sequestering ability of L^{3-} towards M^{2+} was computed by calculating $pL_{0.5}$, a semi-empirical parameter that allows comparisons among different ligands. It represents the antilogarithm of the ligand total concentration required to sequester 50% of the metal cation present at trace level.

Rigorously, $pL_{0.5}$ is not a true constant since it depends on the calculation conditions (pH, ionic strength and temperature), and, mainly, on the analytical concentration of the metal cation (C_M). Especially in the presence of polynuclear M_jL species a general derivation of pL is not straightforward directly from mass balance equations and depends on case to case. However, as C_M tends to 0, $pL_{0.5}$ tends to become a constant. Further details are given in ref [45].

Briefly, the higher the $pL_{0.5}$ value, the greater the sequestering ability. Additional details and applications can be found in references [19,46–52].

Distribution diagrams were drawn by using HySS software [53]. BSTAC [34] program was used for the calculation of equilibrium constants and the other relative parameters. The non-linear least square computer program LIANA [34] was used to fit different equations. ES2WC [34] was used for the calculation of the pure water model approach. Throughout the paper, uncertainties are given as a 95 % confidence interval.

3. Results and discussion

3.1. Acid-base properties of trans-aconitic acid

Protonation constants were fitted analyzing potentiometric titrations (all datapoints are listed in MS Excel Spreadsheet in Supplementary Material) with BSTAC4 software in the molar concentration scale at different ionic strengths, temperatures and in different ionic media, and then converted to molal concentration scale. Since the amount of data is very large, the complete dataset, both in the molar and molal concentration scales, is reported as supplementary material (Table S1). As expected, three protonation constants were obtained (see Table 3). The first protonation constant should be assigned to carboxylate bond to the methylene bridge, whereas the others to the fumarate-like carboxylates.

From the data collected it appeared that the protonation constants values obtained in $(C_2H_5)_4NI$ were higher than those detected in sodium and potassium chloride, with a trend that can be summarized as follows:

Table 3
Parameters obtained fitting stepwise protonation constants to eq. (3) in the molal (SIT) and in the molar (EDH) concentration scales at T = 298.15 K and p = 0.1 MPa.

			Molal concentration scale (SIT)		
			KCl	NaCl	$(C_2H_5)_4NI$
i	$\log {}^{T}K_i^H$	${}^{T}\Delta H^0_{i01}$	$\Delta\varepsilon_{i01}$		
1	6.32 ± 0.01	6.9 ± 0.6	0.174 ± 0.014	0.204 ± 0.018	0.737 ± 0.033
2	4.40 ± 0.01	1.4 ± 0.5	0.216 ± 0.011	0.184 ± 0.026	0.068 ± 0.026
3	2.96 ± 0.01	−0.2 ± 0.4	0.128 ± 0.011	0.122 ± 0.017	−0.02 ± 0.01
			Molar concentration scale (EDH)		
			KCl	NaCl	$(C_2H_5)_4NI$
i	$\log {}^{T}K_i^H$	${}^{T}\Delta H^{0c}_{i01}$	C_{i01}		
1	6.32 ± 0.01	7.0 ± 0.6	0.192 ± 0.014	0.221 ± 0.020	0.912 ± 0.032
2	4.40 ± 0.01	1.5 ± 0.4	0.230 ± 0.012	0.194 ± 0.026	0.127 ± 0.030
3	2.95 ± 0.01	−0.1 ± 0.3	0.159 ± 0.012	0.170 ± 0.026	0.062 ± 0.019

a ± s (standard deviation); standard uncertainties (u): $u(T) = 0.1$ K; $u(p) = 1$ kPa;

$(C_2H_5)_4NI$ > KCl ≈ NaCl. This may be attributed, as expected, to the weaker interaction between tetraalkylammonium cations and carboxylate with respect to sodium and potassium cations [42,54,55]. As an example, in Fig. 1 the trend of the first protonation constant is reported at T = 298.15 K. Similar trends are observed for the other protonation constants even though to a lower extent (*i.e.*, differences are within experimental errors).

The selected set of ligand protonation data was fitted to eq. (3) and a series of parameters useful to calculate $\log K_i^H$ values at any condition (I, T, medium) within experimental domain was obtained (Table 3) both in the molal (SIT) and in the molar (EDH) concentration scales. During the refinement process, it was found that $\Delta\varepsilon'_{ijk}$ parameter resulted not significant at 95% (C.I.), therefore it was fixed at 0 in all cases. Literature about acid-base properties of *trans*-aconitic acid is quite poor, in fact, no recommended data are reported in the most relevant databases [56,57] and only two papers may be considered reliable [30,32]. Kostakis determined the protonation constants in KNO_3 at I = 0.1 mol dm^{-3}, with values of $\log K_1^H = 5.61$, $\log K_2^H = 3.95$, and $\log K_3^H = 2.72$, while Berto in KCl at I = 0.1 mol dm^{-3}, with values of $\log K_1^H = 5.56$, $\log K_2^H = 3.94$, and $\log K_3^H = 2.74$. Values here reported are very close, being 5.67, 3.98 and 2.74 (same order), in KCl at I = 0.1 mol dm^{-3}.

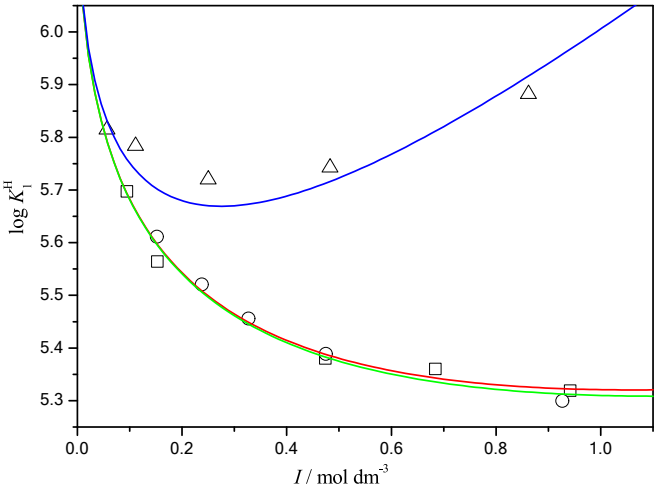

Fig. 1. Dependence of the first protonation constants of trans-aconitate on ionic strength (in mol dm^{-3}) at T = 298.15 K in $(C_2H_5)_4NI_{(aq)}$ (Δ), $KCl_{(aq)}$ (□), $NaCl_{(aq)}$ (○). Solid lines represent the model obtained by eq. (3).

As far as other carboxylate ligands are concerned, the protonation constants of TCA, that has the same structure of aconitic acid but the unsaturation, are remarkably higher than *trans*-aconitate being log K_1^H = 6.45, log K_2^H = 4.91 and log K_3^H = 3.68 (KCl 0.1 mol dm^{-3}). This can be likely interpreted considering the more rigid structure of aconitic acid (only one sp^3 carbon atom out of six) compared to TCA (3 sp^3 carbon atoms and 3 sp^2).

Using the data listed in Table 3 in the molal concentration scale (SIT) for KCl, thermodynamic parameters (ΔG^0, ΔH^0, and $T\Delta S^0$, in kJ mol^{-1}) were calculated at different ionic strength values. The data given in Table 4 reveal that the first protonation step is slightly endothermic, whereas the second and the third are exothermic in all conditions. The main contribution to the proton binding is always entropic in nature for the three protonation steps.

The values of protonation enthalpy changes here found for aconitic acid, namely $^T\Delta H^0_{101}$ = (6.9 ± 0.6) kJ mol^{-1}, $^T\Delta H^0_{201}$ = (1.4 ± 0.4) kJ mol^{-1} and $^T\Delta H^0_{301}$ (-0.2 ± 0.4) kJ mol^{-1}, display a comparable order of magnitude with respect to the ones reported [57] for TCA, *i.e.* $^T\Delta H^0_{101}$ = 3.5 kJ mol^{-1}, $^T\Delta H^0_{201}$ = 4.18 kJ mol^{-1}, $^T\Delta H^0_{301}$ = 0 kJ mol^{-1}. A similar behavior was observed for molecules with the same functional groups [18,47,48,58].

The data analysis performed according to the "Pure Water Model" (eq. (4)) was done with ES2WC software [59]. For this approach only the data reported at T = 298.15 K were used and $(C_2H_5)_4NI$ was selected as the baseline electrolyte. The protonation constants obtained at infinite dilution (Table 3) were kept fixed. Moreover, to avoid correlation between c_0 and c_1 parameters during the refinement, it was chosen to fix the value of c_0 (at c_0 = 0.165) and refine only c_1. This strategy was adopted since the variability of z^*_{ijk} (variable related to c_1) is higher than that of p^*_{ijk} (related to c_0).

The best fit (mean deviation 0.04 in log K units) was obtained refining the equilibrium constants of four weak species, namely NaL^{2-}, $NaHL^-$, KL^{2-} and KHL^-; results are given in Table 5.

Equilibrium constants of the weak species here reported for *trans*-aconitate with Na^+ and K^+ are of the same order of magnitude as other carboxylate with the same charge [60,61]. Despite the relatively low values of such stability constants, their assessment is crucial since in all natural water systems the concentration of alkali metal cations is quite high. Moreover, this information is particularly useful when modeling the chemical speciation in multicomponent solutions, where Na^+ and K^+ coexist. An extensive discussion about this point is reported in ref [54].

Table 4
Thermodynamic parameters ($-\Delta G^0_{i01}$, ΔH^0_{i01}, and $T\,\Delta S^0_{i01}$, in kJ mol^{-1}) for the three *trans*-aconitate protonation steps (i) at different ionic strength values in $KCl_{(aq)}$ and at T = 298.15 K and p = 0.1 MPa.

I [a]	i	$-\Delta G^0_{i01}$	ΔH^0_{i01}	$T\,\Delta S^0_{i01}$
0.15	1	31.9	4.7	36.6
0.15	2	22.4	−0.4	22.1
0.15	3	15.4	−0.9	14.5
0.25	1	31.3	4.3	35.6
0.25	2	22.1	−0.6	21.5
0.25	3	15.3	−1.0	14.2
0.50	1	30.6	3.8	34.4
0.50	2	21.7	−0.9	20.8
0.50	3	15.2	−1.2	14.0
0.75	1	30.2	3.5	33.8
0.75	2	21.7	−1.1	20.5
0.75	3	15.2	−1.3	13.9
1.00	1	30.1	3.3	33.4
1.00	2	21.7	−1.3	20.5
1.00	3	15.3	−1.4	14.0

[a] in mol kg$(H_2O)^{-1}$; standard uncertainties (u): $u(T)$ = 0.1 K; $u(I)$ = 0.01 mol kg^{-1}; $u(p)$ = 1 kPa; $u(\Delta G^0)$ = 0.1 kJ mol^{-1}; $u(\Delta H^0)$ = 1 kJ mol^{-1}; $u(T\Delta S^0)$ = 1 kJ mol^{-1}.

Table 5
Equilibrium constants of the *trans*-aconitate species according to the pure water model at T = 298.15 K and p = 0.1 MPa.

Equilibrium	i	j	k	log $^T\beta_{ijk}$	p^*_{ijk}	z^*_{ijk}	c_0	c_1
$H^+ + L^{3-} = HL^{2-}$	1	0	1	6.315[a]	1	6	0.165[c]	0.13 [d] ± 0.01
$2H^+ + L^{3-} = H_2L^-$	2	0	1	10.711 [a]	2	10	0.165	0.13 ± 0.01
$3H^+ + L^{3-} = H_3L^0$	3	0	1	13.660 [a]	3	12	0.165	0.13 ± 0.01
				log $^T\beta^M_{ijk}$	p^*_{ijk}	z^*_{ijk}	c_0	c_1
$K^+ + L^{3-} = KL^{2-}$	0	1	1	0.83 ± 0.21[b]	1	6	0.165	0.13 ± 0.01
$K^+ + H^+ + L^{3-} = KHL^-$	1	1	1	6.16 ± 0.44[b]	2	10	0.165	0.13 ± 0.01
$Na^+ + L^{3-} = NaL^{2-}$	0	1	1	0.97 ± 0.17[b]	1	6	0.165	0.13 ± 0.01
$Na^+ + H^+ + L^{3-} = NaHL^-$	1	1	1	6.50 ± 0.25[b]	2	10	0.165	0.13 ± 0.01

[a] Taken from Table 3 and kept constant during calculations;
[b] 95 % C.I.;
[c] kept fixed during calculations;
[d] fitted during the fitting of the protonation constants obtained in NaCl, KCl, and $(C_2H_5)_4NI$. Standard uncertainties u are $u(T)$ = 0.1 K, $u(p)$ = 1 Kpa.

3.2. Interaction of trans-aconitic acid with Cd^{2+}, Pb^{2+}, Mn^{2+}

Interaction of *trans*-aconitic acid with Cd^{2+}, Pb^{2+}, Mn^{2+} was studied by means of potentiometric titrations in $KCl_{(aq)}$ at different ionic strength values and at T = 298.15 K. The data analysis was performed using the feature of BSTAC4 computer program to analyze simultaneously titrations carried out at different ionic strength values to obtain formation constants of $M_jH_iL_k$ species together with the relative ionic strength dependence parameters C_{ijk} (using eq. (S6)). Data relative to the protonation constants of L^{3-} in KCl medium (Table 3), as well as those relative to the formation of M^{2+}/OH^- (taken from refs [62,63]) were kept fixed during calculations. On the contrary, the stability constants for M^{2+}/Cl^- complexes were not included; therefore, the retrieved stability constants values here reported are strictly valid only in $KCl_{(aq)}$. Different speciation models were tested, yet the most suitable was selected on the basis of typical selection criteria [64], being also consistent with literature data for similar ligands [65]. The data fitting featured quite low mean deviations (*i.e.*, the average deviation, in absolute value, for all points considered) being 0.6 mV, 0.9 mV, 0.5 mV for Cd^{2+}/L^{3-}, Pb^{2+}/L^{3-} and Mn^{2+}/L^{3-} systems, respectively. These values, expressed in the same unit of measured quantity (e.m.f.) are only slightly higher than the experimental uncertainty (0.2 mV), thus indicating a satisfactory fit. The most reliable speciation model for M^{2+}/L^{3-} systems includes three main species, namely MH_2L^+, $MHL^0_{(aq)}$ and ML^-. However, in the current investigated conditions the formation of species as $Cd_3HL_2^+$ for Cd^{2+}, $Pb(OH)L^-$ for Pb^{2+}, $Mn_3HL_2^+$ and Mn_2HL_2 for Mn^{2+} was evidenced, yet with a low formation percentage (*i.e.* < 5%).

In detail, the results of the data analysis performed in the pH range 2 ≤ pH ≤ 8 are summarized in Table 6, where the formation constant of the species at infinite dilution (log $^T\beta_{ijk}$), the ionic strength dependence parameters (C_{ijk}), the maximum of formation of each species (Max (%)) together with the pH value at which it is achieved (pH_{max}), are listed. Such data may be used to calculate equilibrium constants of those species in $KCl_{(aq)}$ at 298.15 K and up to I = 1.0 mol dm^{-3}. The use of a wider pH range resulted in less reliable fit results, due to the concurrent hydrolysis of the metal cations and precipitation of scarcely soluble hydrolytic species. Nevertheless, for those measurements where precipitation was not observed some tests were performed, but no fitting improvements were achieved, nor species with stoichiometry $M_j(OH)_iL$ were found, except for Pb^{2+}.

As it can be noticed, regardless of the metal cation considered, the equilibrium constants of species with the same stoichiometry are very

Table 6
Overall metal ligand complex formation constants, ionic strength dependence parameters (valid in $KCl_{(aq)}$) in the molar concentration scale, C_{ijk} values and details on the formation percentages (at $I = 0.15$ mol dm^{-3}; analytical concentrations: $C_{Cd} = 1$ mmol dm^{-3}; $C_L = 3$ mmol dm^{-3}) of M^{2+}/L^{3-} species for the selected speciation model obtained in the pH range 2.0 < pH < 8.0 at $T = 298.15$ K and $p = 0.1$ MPa.

Equilibrium	z*	p*	log $^T\beta_{ijk}$	C_{ijk}	Max (%)	pH_{max}
$Cd^{2+} + L^{3-} = CdL^-$	12	1	4.54 ± 0.02 [a]	−0.36 ± 0.06[a]	65	7.0
$Cd^{2+} + H^+ + L^{3-} = CdHL^0_{(aq)}$	14	2	9.94 ± 0.02	0.25 ± 0.03	38	4.6
$Cd^{2+} + 2\,H^+ + L^{3-} = CdH_2L^+$	14	3	13.77 ± 0.01	−0.42 ± 0.05	28	3.0
$3\,Cd^{2+} + H^+ + 2\,L^{3-} = Cd_3HL_2^+$	30	5	19.95 ± 0.07	1.8 ± 0.1	4	5.0
$Pb^{2+} + L^{3-} = PbL^-$	12	1	5.00 ± 0.02	0.97 ± 0.03	69	6.4
$Pb^{2+} + H^+ + L^{3-} = PbHL^0_{(aq)}$	14	2	10.57 ± 0.02	0.34 ± 0.02	46	4.5
$Pb^{2+} + 2\,H^+ + L^{3-} = PbH_2L^+$	14	3	14.81 ± 0.04	−1.36 ± 0.06	46	3.0
$Pb^{2+} + H_2O + L^{3-} = Pb(OH)L^{2-}$	8	0	−4.9 ± 0.1	2.6 ± 0.4	0.6	6.8
$Mn^{2+} + L^{3-} = MnL^-$	12	1	4.97 ± 0.02 [a]	0.68 ± 0.04 [a]	80	6.5
$Mn^{2+} + H^+ + L^{3-} = MnHL^0_{(aq)}$	14	2	10.44 ± 0.02	0.65 ± 0.03	53	4.6
$Mn^{2+} + 2\,H^+ + L^{3-} = MnH_2L^+$	14	3	14.13 ± 0.01	0.37 ± 0. 02	41	3.0
$3\,Mn^{2+} + H^+ + 2\,L^{3-} = Mn_3HL_2^+$	30	5	21.6 ± 0.1	1.2 ± 0.1	4.1	5.1
$2\,Mn^{2+} + H^+ + 2\,L^{3-} = Mn_2HL_2^-$	26	4	17.55 ± 0.08	1.0 ± 0.1	3.2	5.3

[a] s (standard deviation); standard uncertainties: $u(T) = 0.1$ K, $u(p) = 1$ kPa, u(Max) = 1 %; u(pH) = 0.01.

similar as an indication that the complex formation does not depend on the nature of metal cation, even if those reported for Cd^{2+} are slightly lower; C_{ijk} values obtained for Pb^{2+} and Mn^{2+} are higher than those for Cd^{2+}, suggesting that upon increasing chloride concentration *trans*-aconitate would form complexes with Mn^{2+} and Pb^{2+} to a greater extent compared to Cd^{2+}, since the latter interacts with chloride thus leading to a lowering of the conditional formation constant of Cd^{2+}/L^{3-} species. To clarify this behavior, in Figure S1 the difference ($\Delta\log K_{011}$) between the stability constants of ML species (for Cd^{2+}, Pb^{2+} and Mn^{2+}) at various ionic strengths ($\log {}^I K_{011}$) and their corresponding values at infinite dilution ($\log {}^T K_{011}$) is displayed as a function of the ionic strength (KCl). Remarkably, the trend found for CdL^- species is significantly different with respect to the one displayed by the other metal cations, since with the increase of the ionic strength, CdL^- formation constant markedly decreases and, consequently, the difference between cadmium and the other metal cations increases.

The speciation diagrams of the Cd^{2+}/L^{3-} system in Fig. 2 show the different behavior at low ($I = 0.15$ mol kg$(H_2O)^{-1}$, solid line) and at high ionic strength ($I = 1.00$ mol kg$(H_2O)^{-1}$, dashed line) values. In the selected experimental conditions (analytical concentrations: $C_{Cd} = 0.001$ mol kg^{-1}; $C_L = 0.003$ mol kg^{-1}) at $I = 0.15$ mol kg^{-1}, the maximum percentages of formation at $I = 0.15$ mol kg^{-1} are achieved at pH = 3.40 (29 %) for CdH_2L^+, at pH = 4.65 (39 %) for $CdHL^0_{(aq)}$ and at pH > 7.2 (70 %) for CdL^- species. At $I = 1.00$ mol kg$(H_2O)^{-1}$, the maximum formation percentages are found at pH = 3 (4 %) for the CdH_2L^+, at pH = 4.5 (19 %) for $CdHL^0_{(aq)}$ and at pH ~ 7 (15 %) for CdL^- species. At high ionic strength, the formation percentages of the Cd^{2+}/L^{3-} species are quite low, likely as result of the competition between *trans*-aconitate and chloride for the cadmium complexation, also explaining the presence of a relative minimum in the free Cd^{2+} concentration at pH ~ 5. Moreover, at low ionic strength the complexation is shifted to more alkaline pH values (*i.e.*, ~ 0.2 pH units).

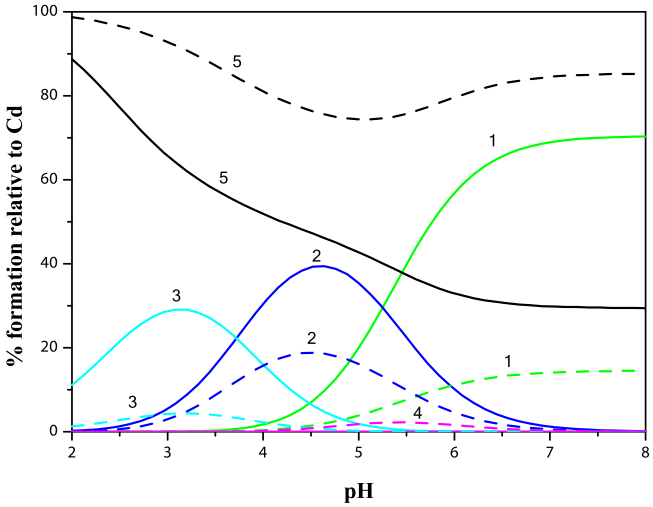

Fig. 2. Speciation diagrams of the Cd^{2+}/L^{3-} system are given at low $I = 0.15$ mol kg^{-1} (solid line) and high ionic strength 1 mol kg^{-1} (dashed line) at $T = 298.15$ K and $p = 0.1$ MPa. Analytical concentrations: $C_{Cd} = 0.001$ mol kg^{-1}; $C_L = 0.003$ mol kg^{-1}. Species: 1 CdL^-, 2 $CdHL^0$, 3 CdH_2L^+, 4 $Cd_3H_2L^+$, 5 free Cd^{2+}.

The speciation diagram of the Pb^{2+}/L^{3-} system is depicted in Fig. 3 in the same experimental conditions. In this case, at $I = 0.15$ mol kg$(H_2O)^{-1}$, the percentage of maximum formation is reached at pH = 3 (69 %) for PbH_2L^+ species, at pH = 4.6 (56 %) for $PbHL^0_{(aq)}$ and at pH ~ 6.5 (80 %) for PbL^- species. At $I = 1.00$ mol kg$(H_2O)^{-1}$, percentages of maximum formation are detected at pH = 3 (4.5 %) for PbH_2L^+, at pH = 4 (41 %) for $PbHL^0_{(aq)}$ and at pH = 6 (80 %) for PbL^- species. In this system, a relevant formation is achieved by the $Pb(OH)^+$ species at pH = 8, namely 55 % and 35%, respectively at $I = 0.15$ and 1.00 mol kg$(H_2O)^{-1}$. As stated, in the selected conditions, $Pb(OH)L^{2-}$ is a minor species.

In the case of Mn^{2+}/L^{3-} system, the distribution diagrams of the species are not strongly affected by ionic strength, very likely due to the negligible impact of the manganese chloride species in the speciation. Accordingly, for all species no substantial difference in the formation percentages can be detected, as represented in Fig. 4. In particular, at $I = 0.15$ mol kg$(H_2O)^{-1}$, maximum formation percentage is reached at pH = 3 (50 %) for MnH_2L^+ species, at pH = 4.5 (63 %) for $MnHL^0_{(aq)}$ and at pH > 7.5 (90 %) for MnL^- species. At $I = 1$ mol kg^{-1}, percentages of

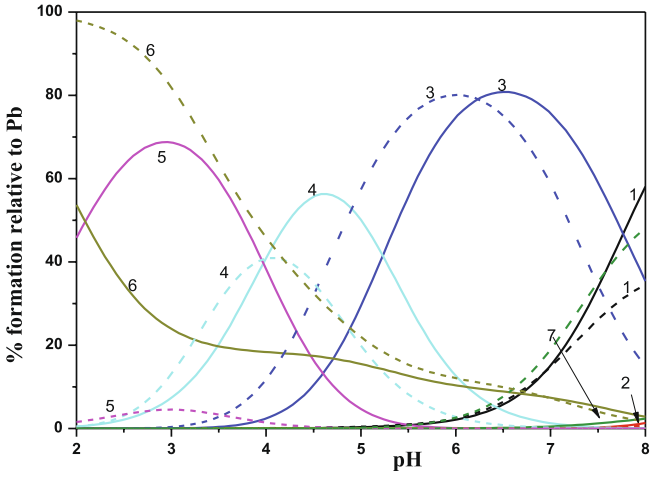

Fig. 3. Speciation diagrams of the Pb^{2+}/L^{3-} system are given at low $I = 0.15$ mol kg^{-1} (solid line) and high ionic strength 1 mol kg^{-1} (dashed line) at $T = 298.15$ K and $p = 0.1$ MPa. Analytical concentrations: $C_{Pb} = 0.001$ mol kg^{-1}; $C_L = 0.003$ mol kg^{-1}. Species: 1 $PbOH^+$, 2 $Pb(OH)_2^0$ 3 PbL^-, 4 $PbHL^0$, 5 PbH_2L^+, 6 free Pb^{2+}, 7 $Pb(OH)L^{2-}$.

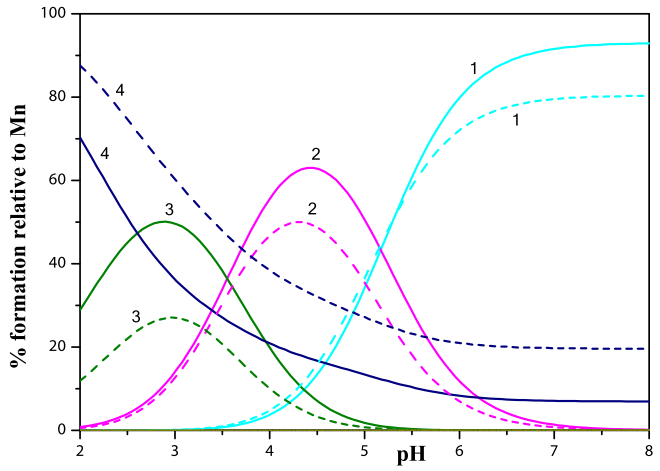

Fig. 4. Speciation diagrams of the Mn^{2+}/L^{3-} system are given at low $I = 0.15$ mol kg^{-1} (black solid line) and high ionic strength 1 mol kg^{-1} (red dashed line) at $T = 298.15$ K and $p = 0.1$ MPa. Analytical concentrations: $C_{Mn} = 0.001$ mol kg^{-1}; $C_L = 0.003$ mol kg^{-1}. Species: 1 MnL^-, 2 $MnHL^0$, 3 MnH_2L^+, 4 free Mn^{2+}. (For interpretation of the references to colour in this figure legend, the reader is referred to the web version of this article.)

maximum formation are detected at pH = 3 (27 %) for MnH_2L^+, at pH = 4.3 (50 %) for $MnHL^0_{(aq)}$ and at pH > 7.5 (80 %) for MnL^- species.

The inclusion of chloride complexes was tested for Cd^{2+}/L^{3-} system according to a pure water model approach. This means considering protonation of *trans*-aconitate and K^+/L^{3-} complexes (see data in Table 5) in a not interacting medium. Moreover, Cd^{2+} hydrolysis and Cd^{2+}/Cl^- in not interacting medium were calculated from literature in ClO_4^- medium [3,66] and are listed in Table S2. In such a way, the analysis of the potentiometric titrations of the Cd^{2+}/L^{3-} system (MS Excel Spreadsheet in Supplementary Material) can be performed in a Pure water model fashion (eq. (4) by fixing c_0 and c_1 values reported in Table 5 also for the CdL^-, $CdHL$ and CdH_2L^+ species, whose log $^T\beta_{ijk}$ values were kept fixed to those listed in Table 6. This allowed the determination of the stability constants of three further quaternary $CdLH_iCl$ species, with the same number of protons as the ternary $CdLH_i$ ones (Table 7).

This result looks plausible if one considers that quite strong Cd^{2+}/Cl^- complexes may lead $CdCl^+$ (other than free Cd^{2+}) to directly interact with differently protonated *trans*-aconitate H_iL. In terms of speciation, the two models (*i.e.*, conditional and pure water) are fully equivalent: the formation percentages of the each CdH_iL species in the conditional model is equivalent to the sum of relative ternary and quaternary species in the pure water model within the uncertainty of the fitted constants

Table 7
Equilibrium constants and ionic strength dependence parameters of the Cd^{2+}/*trans*-aconitate species according to the pure water model at $T = 298.15$ K and $p = 0.1$ MPa.

Equilibrium	i	j	k	log $^T\beta_{ijk}$	p^*_{ijk}	z^*_{ijk}	c_0 [b]	c_1 [b]
$Cd^{2+} + 2\,H^+ + L^{3-} = CdH_2L^+$	2	1	1	13.77 [a]	14	3	0.165	0.13
$Cd^{2+} + H^+ + L^{3-} = CdHL^0_{(aq)}$	1	1	1	9.95 [a]	14	2	0.165	0.13
$Cd^{2+} + L^{3-} = CdL^-$	0	1	1	4.54 [a]	12	1	0.165	0.13
$Cd^{2+} + 2\,H^+ + Cl^- + L^{3-} = CdH_2LCl^0_{(aq)}$	2	1	1	15.70 ± 0.02	16	4	0.165	0.13
$Cd^{2+} + H^+ + Cl^- + L^{3-} = CdHLCl^-$	1	1	1	11.87 ± 0.04	14	3	0.165	0.13
$Cd^{2+} + Cl^- + L^{3-} = CdLCl^{2-}$	0	1	1	6.15 ± 0.04	10	2	0.165	0.13

[a] data from Table 6,
[b] data from Table 5.

(always below 10 %, which can be considered fairly acceptable for so complex systems). For example, at $I = 0.15$ mol dm^{-3}, the formation percentage, fixing $C_M = 1$ mmol dm^{-3} and $C_L = 3$ mmol dm^{-3}, in the conditional model (data of Fig. 2) is 29 % (CdH_2L^+), 39 % ($CdHL^0_{(aq)}$), and 70 % (CdL^-), while in pure water it is 36% (32 % CdH_2L^+ + 4 % $CdH_2LCl^0_{(aq)}$), 49 % (46 % $CdHL^0_{(aq)}$ + 3 % $CdHLCl^-$), and 75 % (68 % CdL^- + 7 $CdLCl^{2-}$); at $I = 1.00$ mol dm^{-3}, the formation percentage in the conditional model (data of Fig. 2) is 4 % (CdH_2L^+), 19 % ($CdHL^0_{(aq)}$), and 15 % (CdL^-), while in pure water it is 12% (only 12 % $CdH_2LCl^0_{(aq)}$), 17 % (only 17 % $CdHLCl^-$), and 25 % (only 25 $CdLCl^{2-}$).

Similar considerations could be done also for Pb^{2+} and Mn^{2+}, even if the importance of chloro complexes for Pb^{2+} is less relevant compared to Cd^{2+} and fairly negligible for Mn^{2+}.

3.3. Literature comparisons

Direct literature comparisons regarding the M^{2+}/L^{3-} systems can be made only for Cd^{2+} and Mn^{2+}.

As far as cadmium is concerned, in the paper of Kostakis *et al.* [30] stability constants were determined in aqueous KNO_3 solution at $I = 0.1$ mol dm^{-3} and at 298.15 K by potentiometric titrations (analytical concentrations: $C_M = C_L = 4$ mmol dm^{-3}). Authors reported the formation of four complex species, namely $CdH_4L^0_{(aq)}$, $Cd_3H_2L_2^{2+}$, $Cd_3HL_2^+$, $Cd_3L_2^0$. By means of ESI-MS and ^{113}Cd NMR measurements, the formation of CdH_4L_2 species was confirmed, whereas the occurrence of the other species was only suggested. In this work, although several tests have been carried out to verify the potential presence of minor or polynuclear species, only the $Cd_3HL_2^+$ species was determined, with a maximum formation percentage of 4 % at pH = 5 at $I = 0.1$ mol dm^{-3}. This may be interpreted considering that in this study the metal to ligand ratio was always in favor of the ligand. Moreover, as shown before, chloride of the ionic medium (KCl) used in this investigation is competing with *trans*-aconitate for Cd^{2+} complexation likely disadvantaging the formation of polynuclear species as, for example, $Cd_3L_2H_i$ determined by Kostakis *et al.* [30].

Regarding the Mn^{2+}/L^{3-} system, Li *et al.* [67] determined the stability of manganous complexes (using $^{54}MnCl_2$) for a series of organic acids by means of ion and solvent extraction. For *trans*-aconitic acid, authors determined log $K = 2.27$ for the MnL^- species at pH = 7.2 – 7.3, $I = 0.16$ mol dm^{-3} (in Veronal buffer, namely sodium diethyl barbiturate and sodium acetate) and $T = 298.15$ K. The cited value likely refers to a Schwarzenbach conditional constant. Computing the same quantity at the same pH and ionic strength values using our dataset, a value of 3.8 is obtained.

Some comparisons of the stability of similar carboxylate ligands with metal cations can also be drawn. For example, TCA has the same structure as *trans*-aconitic except for the absence of the double bond. For TCA, Ajayi *et al.* [68] reported (in $NaClO_4$ at $I = 1$ mol dm^{-3} and $T = 298.15$ K), nine different species for Pb(II), namely PbL^-, PbL_2^{4-}, $Pb_2L_2^{2-}$, $PbHL^+$, $Pb_2HL_2^-$, PbH_2L^+, $PbHL_2^{3-}$, $PbH_3L_2^-$, $Pb_2HL_2^-$ whose formation constants values were 3.17, 4.70, 8.68, 7.9, 14.69, 11.59, 9.96, 18.81 and 13.46, respectively. The comparison of the stability constants of the common species between Ajayi *et al.* and this study is quite satisfying, as in this work log $\beta = 3.57$, 8.11 and 10.65 were found for PbL^-, $PbHL^0$ and PbH_2L^+ species, respectively.

For CA, in which the double bond of *trans*-aconitic acid is saturated with a hydrogen atom and a hydroxyl group, the following values were reported: i) for Mn^{2+}, log $K_{011} = 3.72$ for the ML species ($I = 0.15$ mol dm^{-3} in NaCl and 298.15 K) [69]; ii) for Cd^{2+}, log $K_{011} = 3.71$ and log $K_{111} = 7.85$ for the CdL and $CdHL$ species (at $I = 0.15$ mol dm^{-3} in KNO_3 and 298.15 K) [70], and iii) for Pb^{2+}, log $K_{011} = 4.44$ and log $K_{012} = 5.92$ (at $I = 1.00$ mol dm^{-3} in $NaClO_4$ and $T = 298.15$ K) [57]. Some relevant values critically analyzed by NIST [57], together with the corresponding values computed for *trans*-aconitic acid in the same conditions of ionic strength are reported in Table 8.

As a general trend, citrate complexes are always more stable than

Table 8
Equilibrium constants reported in the literature for various metal cation-ligand systems at different ionic strength values ($T = 298.15$ K, $p = 0.1$ MPa).

Ligand	Mn*L* [c]	Pb*L* [d]	Cd*L* [c]
Trans-aconitic acid[a]	3.75	3.57	3.22
Tricarballylic acid [b]	2.06 [e]	3.17[f]	
Citric acid [b]	3.72 [e]	4.44[f]	3.76 [e]

[a] This work (KCl);
[b] from ref. [57];
[c] $I = 0.1$ mol dm^{-3};
[d] $I = 1.0$ mol dm^{-3};
[e] in NaCl;
[f] in $NaClO_4$.

trans-aconitate ones, that in turn are characterized by a higher formation constant than tricarballylate. If data for citrate were quite easy to explain due to the extra hydroxyl group, the difference in the stability of the complexes between *trans*-aconitate and tricarballylate is less obvious. The presence of unsaturation, as for *trans*-aconitate, generally lowers the affinity of a ligand towards metal cations, as can be easily demonstrated by looking for relevant data of succinic and fumaric acid in dedicated stability constant databases [56,57]. This uncommon behavior may be likely explained considering that the double bond in *trans*-aconitic acid provides a certain rigidity to the molecule so that the coordination towards metal cations may occur in different and peculiar ways. For example, some studies [71,72] claim that *trans*-aconitic acid has an inherent T-shaped structure and multi-coordination modes towards Zn^{2+} and Cu^{2+} whereas, for the coordination of Cd^{2+}, a distorted mog net with tetrahedral nodes has been found [30].

The particularly high affinity of *trans*-aconitate towards metal cations enables the possibility of using it as a complexing agent. Therefore, the sequestering ability of *trans*-aconitate toward Cd^{2+}, Pb^{2+}, Mn^{2+} was assessed by computing $pL_{0.5}$ at different pH values. In Fig. 5, the $pL_{0.5}$ *vs.* pH plot is shown at $I = 1$ mol kg^{-1}. As a common feature, the $pL_{0.5}$ value increases almost linearly up to pH *ca.* 5. At higher pHs, a plateau is reached for Cd^{2+} and Mn^{2+}, whereas in the case of Pb^{2+} an inversion of the trend at pH ~ 6.5 can be clearly observed, due to the beginning of hydrolysis phenomena. This diagram is of great interest, since it shows how Cd^{2+} can be separated from a solution containing also Pb^{2+} and Mn^{2+}. For example, at pH ~ 7, $pL_{0.5} \sim 1.75$ for Cd^{2+} and $pL_{0.5} \sim 3.25$ for Mn^{2+} and Pb^{2+}. This means that in a solution containing the three metal cations at a trace level, the addition of *trans*-aconitate, at an analytical concentration $C_L = 10^{-pL0.5} = 10^{-3.25} = 0.56$ mmol dm^{-3}, would complex 50 % of both Mn^{2+} and Pb^{2+}, but<5 % of Cd^{2+}. This can be demonstrated by inputting altogether the equilibrium constants of the Mn^{2+}/L^{3-}, Cd^{2+}/L^{3-}, Pb^{2+}/L^{3-} systems, $C_L = 0.56$ mmol dm^{-3}, and $C_{Mn} = C_{Cd} = C_{Pb} = 10^{-15}$ mol dm^{-3} in a software able to draw speciation diagrams (*e.g.*, HySS [53], PyES [40], Visual Minteq [73].

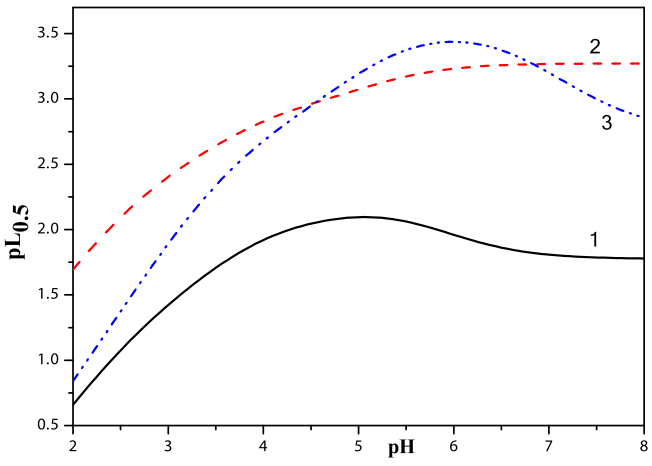

Fig. 5. Dependence of the $pL_{0.5}$ *vs* pH at $I = 1$ mol kg^{-1}, $T = 298.15$ K and $p = 0.1$ MPa, for Cd^{2+} (1) Mn^{2+} (2) and Pb^{2+} (3).

In Fig. 6, the sequestering ability of a series of different complexing agent towards Cd^{2+} is compared by plotting $pL_{0.5}$ values calculated at $T = 298.15$ K and $I = 0.1$ mol dm^{-3} in the pH range $2 \leq pH \leq 8$. As expected, GLDA, bearing 5 binding sites, is characterized by a higher $pL_{0.5}$ than the other complexones, which have different typologies of binding sites, generally result in a strong sequestering ability over a wide pH range. Conversely, molecules such as *trans*-aconitic acid or CA, despite having lower sequestering ability at high pH values, can display $pL_{0.5}$ values comparable to complexones in acidic pH conditions.

This discussion points out once again how the determination of thermodynamic functions, such as equilibrium constants or ionic strength dependence parameters, are the first brick not only for the base chemistry knowledge, but also for many fields of applied chemistry, such as for the modeling of complex matrixes and the design of strategies for remediation purposes.

4. Conclusions

This study is focused on the determination of the thermodynamics of interaction of *trans*-aconitate in aqueous solutions and on the exploration of the suitability of such molecule as an efficient and sustainable sequestering agent towards cadmium, lead and manganese. The results of the study are based on potentiometric titrations performed in different conditions of temperature, ionic strength, and ionic medium. The experimental data obtained (couples of e.m.f. *vs.* titrant added) were analyzed using robust software dedicated to the solution equilibria to obtain equilibrium constants at infinite dilution and useful parameters to model the speciation in different conditions within our experimental domain. The proton binding process resulted to be entropic in nature and enthalpy change values were always close to 0 kJ mol^{-1}. From data collected in different ionic media it was possible to determine the stability of weak species of *trans*-aconitate with Na^+ and K^+; both cations resulted to slightly interact with the ligand and their formation constants are comparable, being log $K = 0.83$ and 0.97 at infinite dilution for the KL^{2-} and NaL^{2-} species, respectively. As far as the interaction with heavy metal cations is concerned, the whole of the data collected on the M^{2+}/L^{3-} systems evidenced the formation of three complex species in the $2 > pH > 8$ range for all the cations considered, namely Cd^{2+}, Mn^{2+} and Pb^{2+}, with stoichiometry ML^{2-}, $MHL^0_{(aq)}$, MH_2L^+. The formation of some

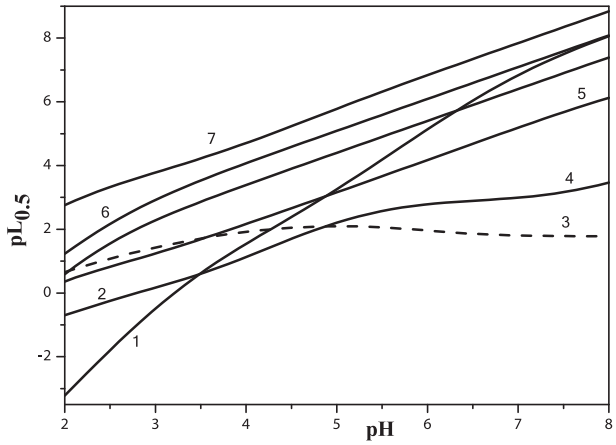

Fig. 6. Comparison of the $pL_{0.5}$ of various complexones towards Cd^{2+} at $I = 0.1$ mol dm^{-3} and $T = 298.15$ K at different pH values. Complexones: S,S-Ethylenediamine-N, N'-disuccinic acid (EDDS) (1), Citric acid (2), *Trans*-aconitic acid (3), N-(2-hydroxyethyl)iminodiacetic acid (HIDA) (4), Nitrilotriacetic acid (NTA) (5), Methylglycindiacetic acid (MGDA) (6), L-glutamic acid N,N-diacetic acid (GLDA) (7).

minor species, such as $Cd_3L_2H^+$, and $Mn_3L_2H^+$ was also hypothesized, but their presence should be proved with dedicated measurements. If in the literature the presence of polynuclear species was demonstrated for Cd(II) by ESI-MS measurements, they were never determined for Mn(II) nor for Pb(II). As this work was performed in aqueous KCl, and data reported are strictly valid in this medium, ionic strength was found to significantly influence the chemical speciation of Cd^{2+}, whereas for Pb^{2+} and Mn^{2+} the presence of chloride does not exert a large effect. Both the presence of polynuclear species and the unusually higher stability of metal cations/*trans*-aconitate complexes compared to the saturated homologue (*i.e.,* TCA) was attributed to a peculiar T-shaped coordination mode, already reported in the literature.

The sequestering ability of *trans*-aconitate towards the three metal cations was estimated by computing the $pL_{0.5}$ values in different conditions of pH and ionic strength values. *Trans*-aconitate resulted a quite good sequestering agent towards the three metal cations, having higher $pL_{0.5}$ values for Mn^{2+} and Pb^{2+} compared to Cd^{2+} (particularly at pH > 5), and featured a similar sequestering ability towards Cd^{2+} with respect to EDTA and S,S-EDDS at pH < 5.

The correct use of $pL_{0.5}$ values may help in the design of strategies for the selective sequestration of metal cations in a multicomponent solution. For example, when the difference in the value of $pL_{0.5}$ of a ligand towards two cations present in the same solution at a trace level exceeds two, that ligand may be regarded to be selective for the metal cation with the highest $pL_{0.5}$ value, when $C_L \sim 10^{-pL0.5}$.

The data here reported are crucial since they can provide key information to identify the best conditions (*i.e.,* pH, medium and ionic strength, etc.) for toxic metals removal in real aqueous systems and to design efficient environmental remediation processes. Moreover, *trans*-aconitic acid can be obtained by the treatment of a waste biomass from the sugar industry, that is a great opportunity to turn a waste in wealth giving a boost towards circular economy.

CRediT authorship contribution statement

Gabriele Lando: Validation, Data curation. **Clemente Bretti:** Methodology, Investigation, Formal analysis, Writing – original draft. **Demetrio Milea:** Software, Data curation, Writing – review & editing. **Concetta De Stefano:** Supervision, Resources, Writing – review & editing. **Olivia Gómez-Laserna:** Project administration, Writing – review & editing. **Paola Cardiano:** Conceptualization, Visualization, Writing – review & editing.

Declaration of Competing Interest

The authors declare that they have no known competing financial interests or personal relationships that could have appeared to influence the work reported in this paper.

Data availability

Data will be made available on request.

Acknowledgements

Prof. Bretti dedicates this paper to his nephew Lorenzo.

Appendix A. Supplementary material

Supplementary data to this article can be found online at https://doi.org/10.1016/j.molliq.2023.122702.

References

[1] R. Sun, Y. Gao, Y. Yang, Leaching of heavy metals from lead-zinc mine tailings and the subsequent migration and transformation characteristics in paddy soil, Chemosphere 291 (2022), 132792, https://doi.org/10.1016/j.chemosphere.2021.132792.
[2] V. Masindi, K.L. Muedi, Environmental contamination by heavy metals, Heavy Metals 10 (2018) 115–132, https://doi.org/10.5772/intechopen.76082.
[3] F. Crea, C. Foti, D. Milea, S. Sammartano, Speciation of cadmium in the environment, Met. Ions Life Sci. 11 (2013) 63–83, https://doi.org/10.1007/978-94-007-5179-8_3.
[4] M. Somani, M. Datta, G.V. Ramana, T.R. Sreekrishnan, Investigations on fine fraction of aged municipal solid waste recovered through landfill mining: Case study of three dumpsites from India, Waste Manag. Res. 36 (2018) 744–755, https://doi.org/10.1177/0734242X18782393.
[5] E. Padoan, C. Romè, N. Mehta, G.A. Dino, D.A. De Luca, F. Ajmone-Marsan, Bioaccessibility of metals in soils surrounding two dismissed mining sites in Northern Italy, Int. J. Environ. Sci. Technol. 18 (2021) 1349–1360, https://doi.org/10.1007/s13762-020-02938-z.
[6] Q. Zhou, N. Yang, Y. Li, B. Ren, X. Ding, H. Bian, X. Yao, Total concentrations and sources of heavy metal pollution in global river and lake water bodies from 1972 to 2017, Glob. Ecol. Conserv. 22 (2020) e00925.
[7] C.K. Schmidt, H.-J. Brauch, Impact of aminopolycarboxylates on aquatic organisms and eutrophication: Overview of available data, Environ. Toxicol. 19 (2004) 620–637, https://doi.org/10.1002/tox.20071.
[8] M. Sillanpää, Environmental fate of EDTA and DTPA, Rev. Environ. Contam. Toxicol. 152 (1997) 85–111, https://doi.org/10.1007/978-1-4612-1964-4_3.
[9] A. Fathollahi, N. Khasteganan, S.J. Coupe, A.P. Newman, A meta-analysis of metal biosorption by suspended bacteria from three phyla, Chemosphere 268 (2021), 129290, https://doi.org/10.1016/j.chemosphere.2020.129290.
[10] R. Li, T. Zhang, H. Zhong, W. Song, Y. Zhou, X. Yin, Bioadsorbents from algae residues for heavy metal ions adsorption: chemical modification, adsorption behaviour and mechanism, Environ. Technol. 42 (2021) 3132–3143, https://doi.org/10.1080/09593330.2020.1723711.
[11] J. Wang, R. Chen, L. Fan, L. Cui, Y. Zhang, J. Cheng, X. Wu, W. Zeng, Q. Tian, L. Shen, Construction of fungi-microalgae symbiotic system and adsorption study of heavy metal ions, Sep. Purif. Technol. 268 (2021), 118689, https://doi.org/10.1016/j.seppur.2021.118689.
[12] M. Negroiu, A.A. Țurcanu, E. Matei, M. Răpă, C.I. Covaliu, A.M. Predescu, C. M. Pantilimon, G. Coman, C. Predescu, Novel Adsorbent Based on Banana Peel Waste for Removal of Heavy Metal Ions from Synthetic Solutions, Materials (Basel) 14 (2021), https://doi.org/10.3390/ma14143946.
[13] A. James, D. Yadav, Valorization of coconut waste for facile treatment of contaminated water: A comprehensive review (2010–2021), Environ. Technol. Innov. 24 (2021), 102075, https://doi.org/10.1016/j.eti.2021.102075.
[14] L. Fu, Y. Liu, Z. Wang, Y. Chen, C. He, Ion Adsorption of Rice Straw to Marine Heavy Metal Polluted Waste Water, J. Coast. Res. (2018) 359–363, https://doi.org/10.2112/SI83-059.1.
[15] F. Ma, C. Peng, D. Hou, B. Wu, Q. Zhang, F. Li, Q. Gu, Citric acid facilitated thermal treatment: An innovative method for the remediation of mercury contaminated soil, J. Hazard. Mater. 300 (2015) 546–552, https://doi.org/10.1016/j.jhazmat.2015.07.055.
[16] K. Wovkulich, M. Stute, B.J. Mailloux, A.R. Keimowitz, J. Ross, B. Bostick, J. Sun, S.N. Chillrud, In Situ Oxalic Acid Injection to Accelerate Arsenic Remediation at a Superfund Site in New Jersey, Environ. Chem. 11 (2014) 525–537, https://doi.org/10.1071/en13222.
[17] I. Pańczuk-Figura, D. Kołodyńska, Biodegradable chelating agent for heavy metal ions removal, Sep. Sci. Technol. 51 (2016) 2576–2585, https://doi.org/10.1080/01496395.2016.1210642.
[18] C. Bretti, R.M. Cigala, C. De Stefano, G. Lando, S. Sammartano, Thermodynamic solution properties of a biodegradable chelant (MGDA) and its interaction with the major constituents of natural fluids, Fluid Phase Equilibr. 434 (2017) 63–73, https://doi.org/10.1016/j.fluid.2016.11.027.
[19] C. Bretti, R.M. Cigala, C. De Stefano, G. Lando, S. Sammartano, Understanding the bioavailability and sequestration of different metal cations in the presence of a biodegradable chelant S, S-EDDS in biological fluids and natural waters, Chemosphere 150 (2016) 341–356, https://doi.org/10.1016/j.chemosphere.2016.02.023.
[20] G. Thierry, Thesis title: Étude de la composition aromatique de mélasse de canne de La Réunion: mise en évidence de précurseurs d'arôme de nature glycosidique: données supplémentaires sur le non-sucre, Département de Chimie, La Réunion, Saint Denis, 2002.
[21] G.O. Bruni, K.T. Klasson, Aconitic Acid Recovery from Renewable Feedstock and Review of Chemical and Biological Applications, Foods 11 (2022), https://doi.org/10.3390/foods11040573.
[22] A. Kanitkar, G. Aita, L. Madsen, The recovery of polymerization grade aconitic acid from sugarcane molasses, J. Chem. Technol. Biotechnol. 88 (2013) 2188–2192, https://doi.org/10.1002/jctb.4084.
[23] J. Qian, F. Quan, F. Zhao, C. Wu, Z. Wang, L. Zhou, Aconitic acid derived carbon dots: Conjugated interaction for the detection of folic acid and fluorescence targeted imaging of folate receptor overexpressed cancer cells, Sens. Actuators B Chem. 262 (2018) 444–451, https://doi.org/10.1016/j.snb.2018.01.227.
[24] Z. Zhang, P. Jiang, D. Liu, S. Feng, P. Zhang, Y. Wang, J. Fu, H. Agus, Research progress of novel bio-based plasticizers and their applications in poly(vinyl chloride), J. Mater. Sci. 56 (2021) 10155–10182, https://doi.org/10.1007/s10853-021-05934-x.
[25] T. Werpy, G. Petersen, National Renewable Energy Lab., Golden, CO (US), 2004. 10.2172/15008859.
[26] W.N. Gilfillan, W.O.S. Doherty, Starch composites with aconitic acid, Carbohydr. Polym. 141 (2016) 60–67, https://doi.org/10.1016/j.carbpol.2015.12.008.

[27] A. Tzereme, E. Christodoulou, G. Kyzas, M. Kostoglou, D. Bikiaris, D. Lambropoulou, Chitosan Grafted Adsorbents for Diclofenac Pharmaceutical Compound Removal from Single-Component Aqueous Solutions and Mixtures, Polymers 11 (2019) 497, https://doi.org/10.3390/polym11030497.

[28] W. Piang-Siong, P. de Caro, A. Marvilliers, X. Chasseray, B. Payet, A. Shum, B. Cheong Sing, Illien, Contribution of trans-aconitic acid to DPPH scavenging ability in different media, Food Chem. 214 (2017) 447–452, https://doi.org/10.1016/j.foodchem.2016.07.083.

[29] S. Wang, M. Wahiduzzaman, C. Martineau-Corcos, G. Maurin, C. Serre, A Microporous Zirconium Metal-Organic Framework Based on trans-Aconitic Acid for Selective Carbon Dioxide Adsorption, Eur. J. Inorg. Chem. 2019 (2019) 2674–2679, https://doi.org/10.1002/ejic.201801284.

[30] G.E. Kostakis, G. Malandrinos, E. Nordlander, M. Haukka, J.C. Plakatouras, Solution and structural studies of the Cd(II) – Aconitate system, Polyhedron 28 (2009) 3227–3234, https://doi.org/10.1016/j.poly.2009.05.008.

[31] Y.-K. Leong, Role of Molecular Architecture of Citric and Related Polyacids on the Yield Stress of α-Alumina Slurries: Inter- and Intramolecular Forces, J. Am. Ceram. Soc. 93 (2010) 2598–2605, https://doi.org/10.1111/j.1551-2916.2010.03777.x.

[32] S. Berto, P.G. Daniele, E. Prenesti, E. Laurenti, Interaction of oxovanadium(IV) with tricarboxylic ligands in aqueous solution: A thermodynamic and spectroscopic study, Inorg. Chim. Acta 363 (2010) 3469–3476, https://doi.org/10.1016/j.ica.2010.06.047.

[33] D.D.A. Perrin W. L. F., Purification of Laboratory Chemicals. 3rd ed., Pergamon Press: Oxford (UK) p 392 1988 Pergamon Press Oxford(UK) 1988.

[34] C. De Stefano, S. Sammartano, P. Mineo, C. Rigano, Marine chemistry-an environmental analytical chemistry approach, Kluwer Academic Publishers (1997) 71–83.

[35] J. Brønsted, Studies on solubility. IV. The principle of the specific interaction of ions, J. Am. Chem. Soc. 44 (1922) 877–898, https://doi.org/10.1021/ja01426a001.

[36] G. Scatchard, Concentrated solutions of strong electrolytes, Chem. Rev. 19 (1936) 309–327, https://doi.org/10.1021/CR60064A008.

[37] E. Guggenheim, J. Turgeon, Specific interaction of ions, J. Chem. Soc. Faraday Trans. 51 (1955) 747–761, https://doi.org/10.1039/TF9555100747.

[38] L. Ciavatta, The specific interaction theory in evaluating ionic equilibria, Ann. Chim. (Rome) 70 (1980) 551.

[39] I. Grenthe, I. Puigdomenech, B. Allard, Modelling in aquatic chemistry, OECD Publishing (1997).

[40] L. Castellino, E. Alladio, S. Bertinetti, G. Lando, C. De Stefano, S. Blasco, E. García-España, S. Gama, S. Berto, D. Milea, PyES – An open-source software for the computation of solution and precipitation equilibria, Chemometr. Intell. Lab. Syst. 239 (2023), 104860, https://doi.org/10.1016/j.chemolab.2023.104860.

[41] F. Crea, C. De Stefano, C. Foti, D. Milea, S. Sammartano, Chelating agents for the sequestration of mercury(II) and monomethyl mercury(II), Curr. Med. Chem. 21 (2014) 3819–3836, https://doi.org/10.2174/0929867321666140601160740.

[42] P.G. Daniele, C. Foti, A. Gianguzza, E. Prenesti, S. Sammartano, Weak alkali and alkaline earth metal complexes of low molecular weight ligands in aqueous solution, Coord. Chem. Rev. 252 (2008) 1093–1107, https://doi.org/10.1016/j.ccr.2007.08.005.

[43] R.M. Pytkowicz, Activity coefficients in electrolyte solutions, Vol. 1, CRC Press, 1979.

[44] R.M. Pytkowicz, Activity coefficients in electrolyte solutions, Vol. 2, CRC Press, 1979.

[45] Ż. Arciszewska, S. Gama, M. Kalinowska, G. Świderski, R. Świsłocka, E. Gołębiewska, M. Naumowicz, M. Worobiczuk, A. Cudowski, A. Pietryczuk, C. De Stefano, D. Milea, W. Lewandowski, B. Godlewska-Żyłkiewicz, Caffeic Acid/Eu(III) Complexes: Solution Equilibrium Studies, Structure Characterization and Biological Activity, Int. J. Mol. Sci. 23 (2022) 888.

[46] C. Bretti, P. Cardiano, A. Irto, G. Lando, D. Milea, S. Sammartano, Interaction of N-acetyl-L-cysteine with Na^+, Ca^{2+}, Mg^{2+} and Zn^{2+}. Thermodynamic aspects, chemical speciation and sequestering ability in natural fluids, J. Mol. Liq. 319 (2020), https://doi.org/10.1016/j.molliq.2020.114164.

[47] C. Bretti, R.M. Cigala, C. De Stefano, G. Lando, S. Sammartano, Thermodynamic study on polyaspartic acid biopolymer in solution and prediction of its chemical speciation and bioavailability in natural fluids, J. Mol. Liq. 274 (2019) 68–76, https://doi.org/10.1016/j.molliq.2018.10.067.

[48] C. Bretti, C. De Stefano, C. Foti, S. Sammartano, Total and Specific Solubility and Activity Coefficients of Neutral Species of $(CH_2)2_i$–$2N_i(CH_2COOH)_i^{+2}$ Complexons in Aqueous NaCl Solutions at Different Ionic Strengths, ($0 \leq I \leq 5$) mol·L^{-1}, and 298.15 K, J. Chem. Eng. Data 56 (2011) 437–443, https://doi.org/10.1021/je100797b.

[49] P. Cardiano, C. Foti, O. Giuffrè, On the interaction of N-acetylcysteine with Pb^{2+}, Zn^{2+}, Cd^{2+} and Hg^{2+}, J. Mol. Liq. 223 (2016) 360–367, https://doi.org/10.1016/j.molliq.2016.08.050.

[50] P. Cardiano, F. Giacobello, O. Giuffrè, S. Sammartano, Thermodynamics of Al^{3+}-thiocarboxylate interaction in aqueous solution, J. Mol. Liq. 222 (2016) 614–621, https://doi.org/10.1016/j.molliq.2016.07.077.

[51] F. Crea, C. De Stefano, A. Irto, G. Lando, S. Materazzi, D. Milea, A. Pettignano, S. Sammartano, Understanding the Solution Behavior of Epinephrine in the Presence of Toxic Cations: A Thermodynamic Investigation in Different Experimental Conditions, Molecules 25 (2020) 511, https://doi.org/10.3390/molecules25030511.

[52] A. Irto, P. Cardiano, K. Chand, R.M. Cigala, F. Crea, C. De Stefano, G. Gattuso, S. Sammartano, M.A. Santos, Complexation of environmentally and biologically relevant metals with bifunctional 3-hydroxy-4-pyridinones, J. Mol. Liq. 319 (2020), 114349, https://doi.org/10.1016/j.molliq.2020.114349.

[53] L. Alderighi, P. Gans, A. Ienco, D. Peters, A. Sabatini, A. Vacca, Hyperquad simulation and speciation (HySS): a utility program for the investigation of equilibria involving soluble and partially soluble species, Coord. Chem. Rev. 184 (1999) 311–318, https://doi.org/10.1016/S0010-8545(98)00260-4.

[54] C. Bretti, R. Di Pietro, P. Cardiano, O. Gomez-Laserna, A. Irto, G. Lando, C. De Stefano, Thermodynamic solution properties of a biodegradable chelant (L-glutamic-N, N-diacetic acid, l-glda) and its sequestering ability toward $C^{d2}+$, Molecules 26 (2021) https://doi.org/10.3390/molecules26237087.

[55] C. Bretti, C. De Stefano, F.J. Millero, S. Sammartano, Modeling of protonation constants of linear aliphatic dicarboxylates containing -S-groups in aqueous chloride salt solutions, at different ionic strengths, using the SIT and pitzer equations and empirical relationships, J. Solution. Chem. 37 (2008) 763–784, https://doi.org/10.1007/s10953-008-9273-3.

[56] P. May, K. Murray, Joint expert speciation system, JESS Primer, Murdoch Western Australia (2000), https://doi.org/10.1016/0039-9140(91)80289-c.

[57] A. Martell, R. Smith, R. Motekaitis, NIST standard reference database 46, vers. 8, US Department of Commerce, Gaithersburg, Md, USA (2004). 10.18434/T4D303.

[58] C. Bretti, F. Crea, C. Rey-Castro, S. Sammartano, Interaction of acrylic-maleic copolymers with H^+, Na^+, Mg^{2+} and Ca^{2+}: Thermodynamic parameters and their dependence on medium, React. Funct. Polym. 65 (2005) 329–342, https://doi.org/10.1016/j.reactfunctpolym.2005.07.005.

[59] A. De Robertis, C. De Stefano, S. Sammartano, C. Rigano, The determination of formation constants of weak complexes by potentiometric measurements: experimental procedures and calculation methods, Talanta 34 (1987) 933–938, https://doi.org/10.1016/0039-9140(87)80132-7.

[60] C. Bretti, O. Giuffrè, G. Lando, S. Sammartano, Solubility, protonation and activity coefficients of some aminobenzoic acids in $NaCl_{aq}$ and $(CH_3)_4NCl_{aq}$, at different salt concentrations, at T = 298.15 K, J. Mol. Liq. 212 (2015) 825–832, https://doi.org/10.1016/j.molliq.2015.10.043.

[61] F. Crea, C. De Stefano, C. Foti, G. Lando, D. Milea, S. Sammartano, Alkali Metal Ion Complexes with Phosphates, Nucleotides, Amino Acids, and Related Ligands of Biological Relevance. Their Properties in Solution, Met. Ions, Life Sci. 16 (2016) 133–166, https://doi.org/10.1007/978-3-319-21756-7_5.

[62] C. Foti, G. Lando, F.J. Millero, S. Sammartano, Experimental study and modelling of inorganic Cd^{2+} speciation in natural waters, Environ. Chem. 8 (2011) 320–331, https://doi.org/10.1071/EN10138.

[63] P.L. Brown, C. Ekberg, Hydrolysis of Metal Ions, Wiley-VCH Verlag GmbH and Co. KGaA, Weinheim, 2016.

[64] F. Crea, D. Milea, S. Sammartano, Enhancement of hydrolysis through the formation of mixed hetero-metal species, Talanta 65 (2005) 229–238, https://doi.org/10.1016/j.talanta.2004.06.014.

[65] R.M. Smith, A.E. Martell, in: Critical Stability Constants: Second Supplement, Springer, US, Boston, MA, 1989, pp. 299–359.

[66] K.J. Powell, P.L. Brown, R.H. Byrne, T. Gajda, G. Hefter, A.K. Leuz, S. Sjöberg, H. Wanner, Chemical speciation of environmentally significant metals with inorganic ligands. Part 4: The Cd^{2+} + OH^-, Cl^-, CO_3^{2-}, SO_4^{2-}, and PO_4^{3-} systems (IUPAC Technical Report), Pure Appl. Chem. 83 (2011) 1163–1214.

[67] N.C. Li, W.M. Westfall, A. Lindenbaum, J.M. White, J. Schubert, Manganese-54, Uranium-233 and Cobalt-60 Complexes of Some Organic Acids1, J. Am. Chem. Soc. 79 (1957) 5864–5870, https://doi.org/10.1021/ja01579a007.

[68] S.O. Ajayi, A. Olin, P. Svanstrom, A potentiometric titration study of the complex formation between Pb^{2+} and 1,2,3-propanetricarboxylic acid, Acta Chem. Scand. 33 (1979) 93–96.

[69] J.S. Wiberg, On the mechanism of metal activation of deoxyribobuclease I, Arch. Biochem. Biophys. 73 (1958) 337–358, https://doi.org/10.1016/0003-9861(58)90280-7.

[70] S. Capone, A. De Robertis, C. De Stefano, S. Sammartano, Formation and stability of zinc(II) and cadmium(II) citrate complexes in aqueous solution at various temperatures, Talanta 33 (1986) 763–767, https://doi.org/10.1016/0039-9140(86)80184-9.

[71] M.-S. Wang, G.-C. Guo, M.-L. Fu, L. Xu, L.-Z. Cai, J.-S. Huang, Self-assembly of copper(ii) complexes with ladder, bi-rack, rack–ladder–rack and layer structures by the directional-bonding approach using a T-shaped ligand, Dalton Trans. (2005) 2899–2907, https://doi.org/10.1039/B501782C.

[72] G.E. Kostakis, E. Nordlander, N. Hadjiliadis, M. Haukka, J.C. Plakatouras, Two 3D supramolecular architectures from zinc hydrogen aconitate 1D polymers, Inorg. Chem. Commun. 9 (2006) 915–919, https://doi.org/10.1016/j.inoche.2006.05.031.

[73] J.P. Gustafsson, KTH Royal Institute of Technology, Stockholm, Sweden, 2008.